INTERNATIONAL RESEARCH JOURNAL OF ENGINEERING & APPLIED SCIENCES
ISSN: 2322-0821(O) ISSN: 2394-9910(P)
VOLUME 13 ISSUE 4
Oct 2025 - Dec 2025
www.irjeas.org

Research Article

Preliminary CFD Evaluation of Selected Hypotheses for a Wind Energy Concentrator

Tarun Kumar Ahirwar[1], Paulami Sahu[2]*, Prashant V. Baredar[3]

[1] PhD Scholar, School of Environment and Sustainable Development, Central University of Gujarat, India
tarun.9425036057@gmail.com
[2] Asst. Professor, School of Environment and Sustainable Development, Central University of Gujarat, India
paulami_sahu@cug.ac.in
[3] Professor & Head, Department of Energy, Maulana Azad National Institute of Technology, M.P., India
prashant.baredar@gmail.com

*Corresponding Author: paulami_sahu@cug.ac.in

DOI–10.55083/irjeas.2025.v13i04001

Abstract: This paper presents a preliminary computational fluid dynamics (CFD) assessment of four conical frustum windconcentrator configurations (Models A–D) intended for augmentation of small wind turbines in low-wind-speed regions. The designs share a fixed 3:1 inlet-to-outlet area ratio and differ only in frustum length and wall angle, providing a controlled comparison of geometric effects. Steady Reynolds-averaged Navier–Stokes (RANS) simulations with the Realizable k-ε model in ANSYS Fluent quantify outlet velocity amplification (V_Amp = V_out / V_in), radial uniformity and turbulence kinetic energy (TKE). Model B (short and steep taper) achieves the highest V_Amp, whereas longer designs (Models C and D) yield more uniform outflow at the expense of reduced gain. Model A strikes an intermediate balance. The results establish clear geometry–performance trade-offs that are practically relevant: overly high tapers risk non-uniform, turbulent outflow, while long ducts add material and drag but offer diminishing returns. This paper includes only the preliminary interpretation derived from test-run CFD observations. These CFD trends form the basis for turbineintegrated modeling and controlled experimentation in subsequent work.

Keywords: Wind concentrator; Conical frustum; CFD; Amplification; Turbulence; Low-wind sites

1. INTRODUCTION

Small wind turbines (SWTs) in low-wind regions often operate near or below cut-in, depressing annual energy yield and project economics. A practical alternative to taller towers or site relocation is to concentrate the approaching flow so that axial velocity at the rotor plane increases. While ideal power scales as $P \propto \frac{1}{2}\rho A v^3$, real gains are bounded by aerodynamic limits and losses introduced by any guiding structure (wall friction, separation, and turbine–duct interactions) (Vaz& Wood, 2018). Among manufacturable options for micro-turbines, straight conical frusta (contracting nozzles) are proposed because they exchange geometric simplicity and structural stiffness for controllable flow guidance (Mohanan et al., 2021; Shonhiwa and Makaka, 2016).

Designing such concentrators is inherently multi-objective. Short, steep tapers can yield high local acceleration but often at the cost of non-uniform, more turbulent outflow (Masukume et al., 2014); longer passages can smooth the exit profile and reduce peak turbulence kinetic energy (TKE) but add surface area, massand viscous losses—typically with diminishing returns once a target area ratio is achieved (Vaz& Wood, 2018; Taghinezhad et al., 2023). Much of the literature varies several geometric degrees of freedom simultaneously (length, taper, lip radius, inlet/outlet diameters), complicating attribution. To provide a controlled mapping from geometry to performance, the present study fixes the inlet-to-outlet area ratio at 3:1 and varies only frustum length (and implied wall angle) across four hypotheses (Models A–D). Three outlet-plane diagnostics are emphasized because they directly inform rotor integration: velocity amplification $V\_amp=V\_out/V\_in$, radial uniformity and peak outlet-plane TKE.

Computationally, we adopt steady RANS with the Realizable k–ε model and enhanced wall treatment as a robust baseline for internal, mildly separated subsonic flows; k–ω SST is recognized as a useful comparator near adverse pressure gradients and separation (Shih et al., 1995; Menter, 1994, Nouhaila, O. et al.,2024).The objective here is a concise, mesh-independent screening that isolates length/taper effects at fixed area ratio and establishes defensible trends to guide turbine-integrated CFD for controlled experiments.

2. REVIEW OF LITERATURE

Reviews and parametric studies consistently show that guided-inflow devices (diffusers or concentrators) can raise local rotor-plane velocity and improve net performance when system losses are managed; however, the benefit is context-dependent and sensitive to geometry and operating envelope (Vaz& Wood, 2018). System-level intakes such as INVELOX

demonstrate that capture-to-rotor flow management is viable for low-wind environments, albeit with added structural complexity (Allaei&Andreopoulos, 2014). For small-scale implementations, compact conical sections have shown practical gains while keeping fabrication demands modest (Mohanan et al., 2021).

Geometry–performance, Optimization and CFD-based design studies indicate that high contraction increases V_amp but can degrade uniformity and elevate TKE, while longer ducts improve flow quality at the expense of higher wetted area and friction (Vaz& Wood, 2018). Multi-objective frameworks (e.g., CFD coupled with response-surface methodology) typically balance speed-up against pressure loss and flow quality, reinforcing the need to report joint metrics rather than a single headline number (Taghinezhad et al., 2023).

Modeling choices and verification for nozzle-like internal flows, steady RANS remains common in early-stage screening; the Realizable k–ε closure is frequently preferred over the standard form for improved realizability and robustness, while k–ω SST is favored near strong adverse gradients (Shih et al., 1995; Menter, 1994).

3. RESEARCH GAP

Rarely, any studies has explicitly isolated frustum length/taper at fixed area ratio for axisymmetric conical concentrators sized to micro-turbine rotors and joint reporting of V_ampand peak TKE on a common outlet plane is limited. The present work attempts to partly fill this gap by fixing 3:1 area ratio, varying length only for reporting a compact set of screening metrics to inform turbine-integrated modeling and experiments (Vaz& Wood, 2018; Taghinezhad et al., 2023; Wood, 2011).

4. METHODOLOGY

All four models share an outlet diameter D_o = 1.274 m (coincident with the intended rotor plane) and an inlet diameter D_i = 2.206 m, giving a fixed contraction A_i/A_o = 3.0. The frustum wall is a straight generator line (linear taper); only the length L varies across Models A–D to isolate length/taper effects at constant area ratio. Axisymmetry is used for this screening phase to reduce computational load while retaining the principal physics of an axisymmetric contraction (Wood, 2011). Domain extents and symmetry follow low-speed tunnel practice to avoid blockage and recirculation artefacts (Mehta & Bradshaw, 1979; Barlow et al., 1999; Kulkarni &Bewsher, 2011; Azzawi et al., 2016).

Meshing and near-wall resolution

A curvature-based unstructured core (tetra/polygons) is generated with inflation (prism) layers on all solid walls to resolve the boundary layer. Base edge length in the near-field is ~0.05 m, with targeted refinements at (i) the outlet lip and immediate downstream shear layer and (ii)

regions of strong gradients identified from a pilot run. The prism stack uses 12–15 layers, initial height chosen for enhanced wall treatment under the Realizable k–ε model, growth rate ≤ 1.2, yielding wall coordinates y+ ≈ 30–100 over most of the frustum (Shih et al., 1995).

Boundary conditions and fluid properties

The inlet imposes a uniform axial velocity $V_{in} = 3.0$ m s^{-1}, representative of low-wind operation. Turbulence intensity is set to 5%, consistent with conditioned low-speed tunnels or modestly disturbed on-site inflow after honeycomb/screen packs (Mehta & Bradshaw, 1979; Kulkarni &Bewsher, 2011). Air is incompressible with $\varrho = 1.225$ kg m^{-3}; walls are no-slip. The outlet is a pressure outlet at ambient static pressure with backflow turbulence equal to inlet values. The outlet plane is placed ≥ $10D_o$ downstream; shifting it by ±5 m changes V_{amp} by < 1%.

Solver and numerics

Simulations use ANSYS Fluent (pressure-based, steady RANS). The Realizable k–ε closure with enhanced wall treatment is adopted for robustness on internal, mildly separated, subsonic flows (Shih et al., 1995). Spatial discretization is second-order upwind for momentum and turbulence scalars; pressure–velocity coupling uses SIMPLE with body-force-weighted pressure interpolation. Convergence requires scaled residuals ≤ 10^{-6} and a flat area-averaged outlet-velocity monitor (change < 0.1% over 500 iterations). A spot-check with k–ω SST on Model B (fine mesh) changed V_{amp} by ~2% and slightly raised peak TKE near the lip, consistent with SST behaviour in adverse-gradient regions (Menter, 1994).

Post-processing and metrics

All diagnostics are evaluated on the outlet (rotor) plane: • Velocity amplification: $V_{amp} = \bar{V}_{out} / V_{in}$, with $\bar{V}_{out}$ the area-averaged axial velocity over the outlet disk. • Radial uniformity: normalized standard deviation $\sigma_u / \bar{u}$ over the outlet disk; in addition, band-averaged velocities are reported for three radial bands—center, mid-radius and near-wall—to reveal annular high-speed regions. • Flow-quality proxy: peak outlet-plane TKE is recorded as a qualitative indicator of unsteadiness relevant to loads/noise; dedicated aeroacoustics is deferred. Streamlines and wall static pressure are inspected to exclude gross internal separation. Sampling locations, band widths, and averaging scripts are identical across A–D to ensure comparability. Figure 1 depicts the workflow used in the present CFD study.

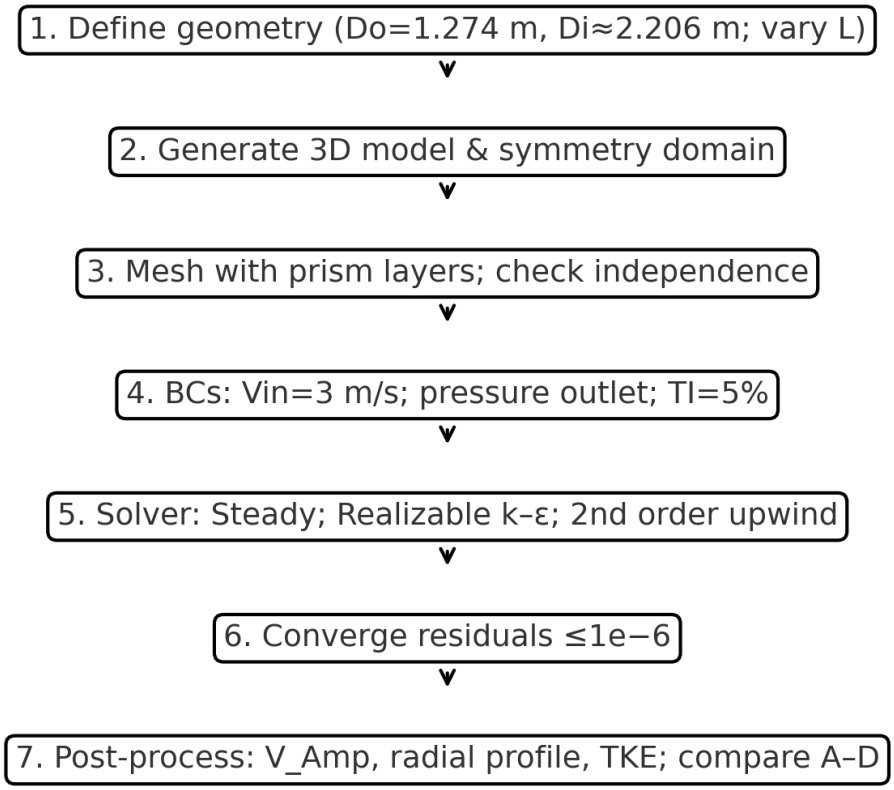

Figure 1. CFD workflow used in present study.

The geometric configurations of tested hypotheses from A to D are tabulated in table 1.

Table 1: Geometric Summary of Models A–D

Model	L (m)	Wall angle (deg)	Surface area (m^2)
Model A	0.999	25.00	7.301
Model B	0.466	45.00	5.160
Model C	3.000	8.83	16.066
Model D	2.206	11.93	12.549

5. RESULTS AND DISCUSSION

3.1 Amplification (V_Amp) across Models A–D:

Amplification (V_Amp) across Models A–Dreveals that Model B (short, steeper taper) exhibits (Fig. 2) the highest amplification due to stronger pressure drop along the converging passage. Model A, with a milder angle, achieves slightly lower V_Amp but displays better outflow behavior. Models C and D (longer frusta) approach the area-ratio ceiling; once the 3:1 contraction is realized, further length adds wall area and friction more than additional acceleration.

3.2 Outlet radial profiles and flow uniformity:

Figure 2. CFD-predicted amplification (V_Amp) for Models A–D.

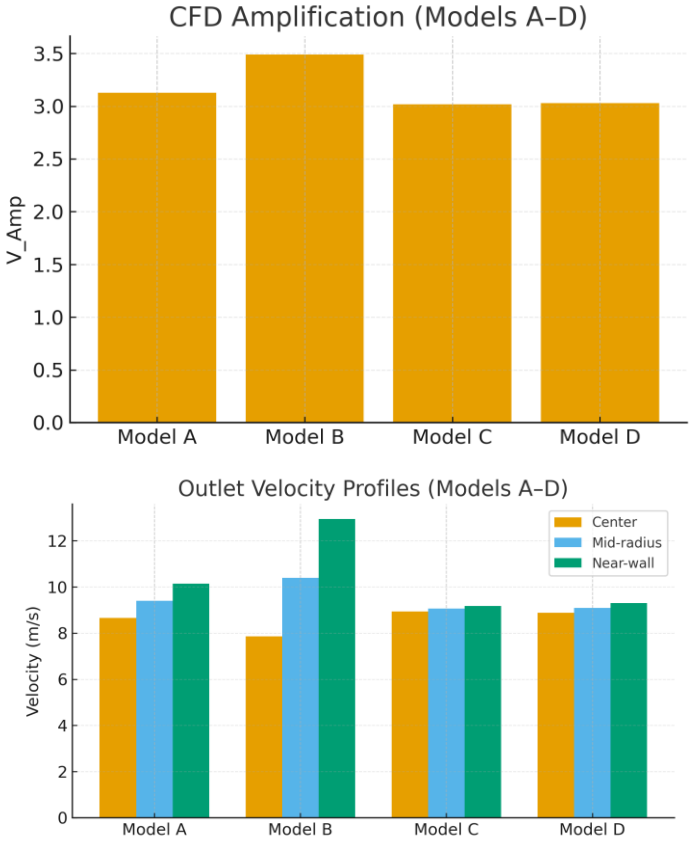

Figure 3. Radial outlet velocity distributions for A–D (center, mid-radius, near-wall).

Short and steep geometries (Fig. 3) tend to produce an annular high-speed region near the wall, while the centerline lags, indicating a shear layer that may adversely affect turbine loading and noise. Longer designs spread acceleration over distance and yield more uniform profiles. A

practical design benefits from both adequate V_Amp and acceptable uniformity.

3.3 *Turbulence kinetic energy (TKE) as a flow-quality indicator:*

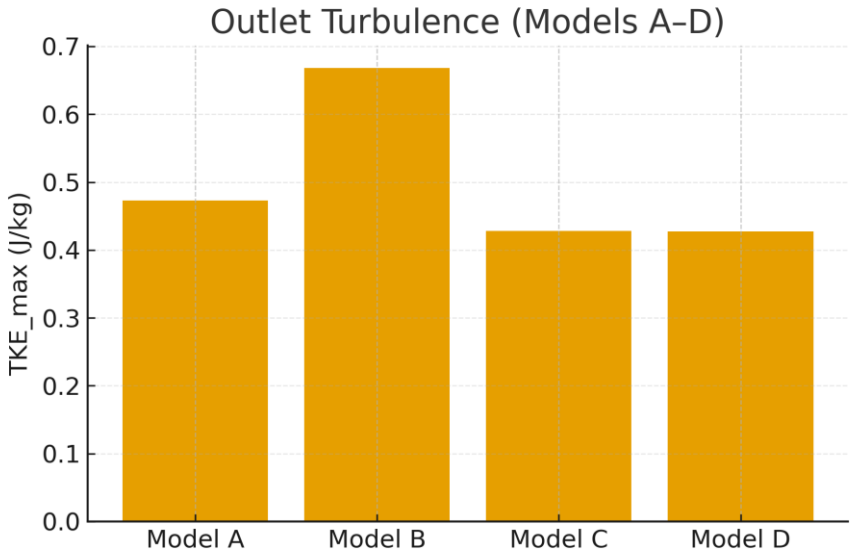

Figure 4. Maximum outlet-plane TKE for Models A–D.

TKE (Fig. 4) provides a qualitative representation for unsteadiness and potential for increased acoustic emissions. Model B's higher V_Amp is accompanied by higher TKE, whereas Models C and D demonstrate lower TKE, consistent with their smoother profiles. Model A offers a balance between amplification and turbulence.

CFD contours were produced during the test runs that informed the quantitative graphs. Among these, Figure 5 presents the outlet-plane velocity contours for Hypothesis Cand Figure 6 presents those for Hypothesis D. These visualizations correspond to the mesh-independent datasets used to compute velocity amplification, radial uniformity, and peak TKE at the rotor plane, and are included here for completeness and traceability to the plotted results. For Hypotheses A and B, their graphs (based on mesh-independent metrics) are already reflected in the results.

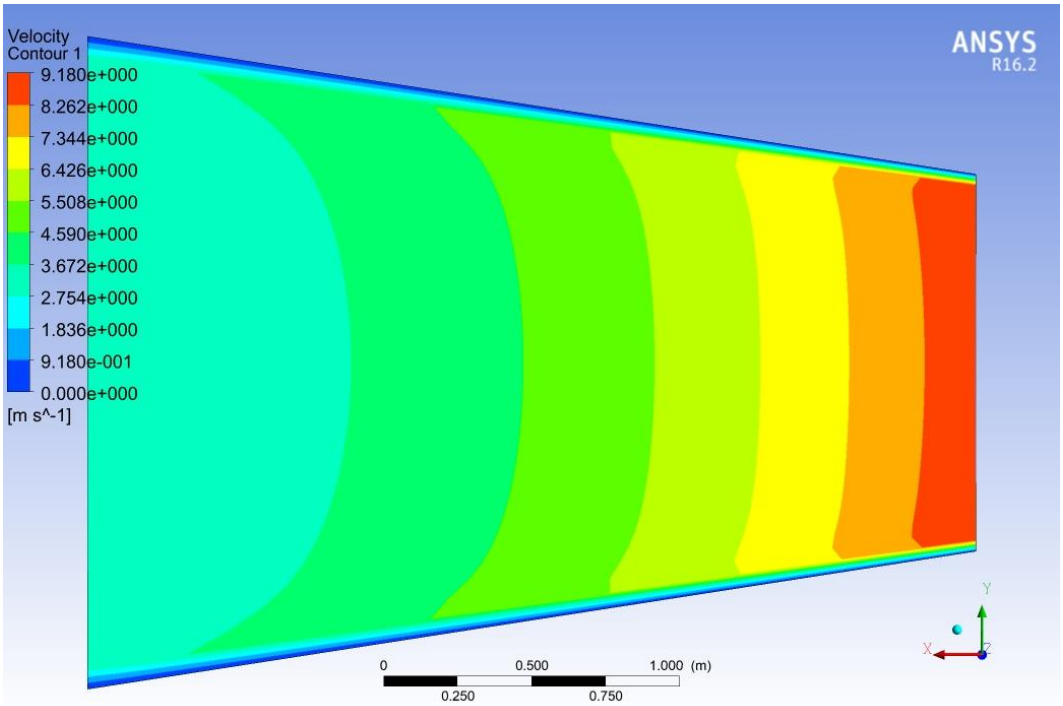

Figure 5. Velocity Contour for Hypothesis C (L = 3.000 m; Realizable k–ε; V_in = 3.0 m s^{-1}).

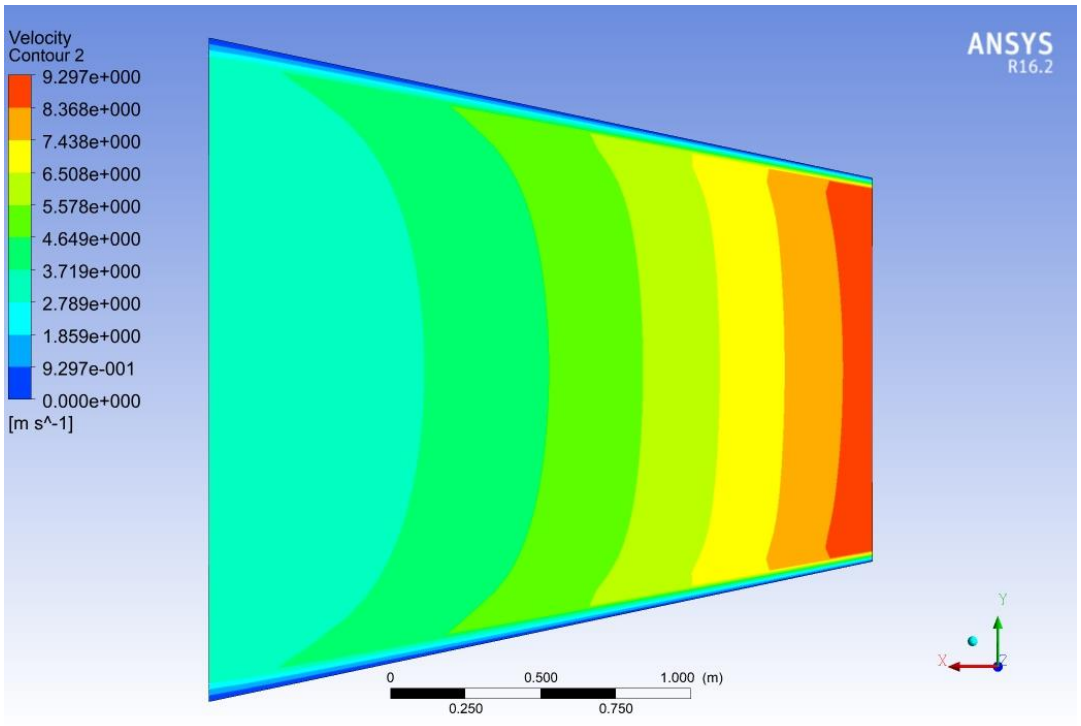

Figure 6. Velocity Contours for Hypothesis D (L = 2.206 m; Realizable k–ε; V_in = 3.0 m s^{-1}).

6. CONCLUSION

This study presented a preliminary test-CFD screening of four axisymmetric conical-frustum concentrators (Models A–D) at a fixed inlet-to-outlet area ratio of 3:1, varying only the frustum length (and implied wall angle). By evaluating outlet-plane velocity amplification (V_amp), radial uniformity (σ_u/ū), and peak turbulence kinetic energy (TKE) on mesh-independent solutions, we established a clear performance robustness trade-off. The short, steep-taper geometry (Model B) delivered the highest V_amp but also showed the least uniform outflow and the largest peak TKE at the rotor plane, implying greater sensitivity of blade loading and potential for unsteadiness. The longer geometries (Models C and D) produced smoother, more uniform outflow with lower peak TKE, yet offered only modest additional acceleration beyond what is already realized by the geometric contraction. Model A, with intermediate length/taper, consistently balanced these competing objectives and is therefore a practical baseline for early integration.

These findings reinforce contemporary design guidance that neither extreme—excessively short/steep nor overly long—tends to be optimal. Instead, the useful design space is bounded by (i) diminishing returns in acceleration once the contraction is realized and (ii) the need to preserve flow quality at the rotor plane. The quantitative trends reported here are acceptable across mesh levels, inlet turbulence variations and reasonable outlet-placement changes, which supports their use as screening evidence prior to higher-fidelity modeling(Vaz& Wood, 2018; Taghinezhad et al., 2023; Werle&Presz, 2008; Celik et al., 2008)..

The ongoing and planned steps includerepeated experimental validation in conditioned low-speed facilities to benchmark absolute levels and confirm uniformity trends and design-for-deployment checks on mass, manufacturability and mounting to translate the favored geometries into field-ready specifications. While full aeroacoustics analysis and comprehensive 3D asymmetry studies are outside the present scope, the lower TKE and smoother profiles of Models C and D suggest promising noise and fatigue characteristics that merit dedicated follow-up. Overall, the study provides a preliminary, self-contained contribution that clarifies geometry–performance trade-offs for concentrator-augmented small wind systems and offers a disciplined foundation for future progression to turbine-coupled CFD and controlled experiments.

REFERENCES

1. Allaei, D., &Andreopoulos, Y. (2014). INVELOX: Description of a new concept in wind power

and its performance evaluation. *Energy, 69*, 336–344. https://doi.org/10.1016/j.energy.2014.03.021

2. Azzawi, I. D. J., Mao, X., & Jaworski, A. J. (2016). Design, fabrication and characterization of a low-speed open-jet wind tunnel. In *Proceedings of the World Congress on Engineering 2016* (Vol. II, pp. 552–557). Newswood Limited. https://eprints.whiterose.ac.uk/99364/
3. Barlow, J. B., Rae, W. H., Jr., & Pope, A. (1999). *Low-speed wind tunnel testing* (3rd ed.). Wiley.
4. Celik, I. B., Ghia, U., Roache, P. J., Freitas, C. J., Coleman, H., &Raad, P. E. (2008). Procedure for estimation and reporting of uncertainty due to discretization in CFD applications. *Journal of Fluids Engineering, 130*(7), 078001. https://doi.org/10.1115/1.2960953
5. Kulkarni, V., &Bewsher, S. (2011). Simulation of honeycomb–screen combinations for improved flow quality in subsonic tunnels. *Journal of Wind Engineering and Industrial Aerodynamics, 99*(10), 1031–1040. https://doi.org/10.1016/j.jweia.2010.10.006
6. Mehta, R. D., & Bradshaw, P. (2016). Design rules for small low-speed wind tunnels. *The Aeronautical Journal, 83*(827), 443–453. https://doi.org/10.1017/S0001924000031985
7. Masukume, P.-M., Makaka, G. and Tinarwo, D. (2014) 'Technoeconomic Analysis of Ducted Wind Turbines and Their Slow Acceptance on the Market', *Journal of Renewable Energy*, 2014, pp. 1–5. https://doi.org/10.1155/2014/951379
8. Menter, F. R. (1994). Two-equation eddy-viscosity turbulence models for engineering applications. *AIAA Journal, 32*(8), 1598–1605. https://doi.org/10.2514/3.12149
9. Mohanan, J. N., Sundaramoorthy, K., & Sankaran, A. (2021). Performance improvement of a low-power wind turbine using conical sections. *Energies, 14*(17), 5233. https://doi.org/10.3390/en14175233
10. Nouhaila, O., Hassane, M., Scutaru, M. L., &Jelenschi, L. (2024). On the accuracy of turbulence model simulations of the exhaust manifold. *Applied Sciences, 14*(12), 5262. https://doi.org/10.3390/app14125262
11. Shih, T.-H., Liou, W. W., Shabbir, A., Yang, Z., & Zhu, J. (1995). A new k–ε eddy-viscosity model for high Reynolds number turbulent flows. *Computers & Fluids, 24*(3), 227–238.

https://doi.org/10.1016/0045-7930(94)00032-T
12. Shonhiwa, C. and Makaka, G. (2016) 'Concentrator Augmented Wind Turbines: A review', *Renewable and Sustainable Energy Reviews*, 59, pp. 1415–1418. https://doi.org/10.1016/j.rser.2016.01.067
13. Taghinezhad, J., Abdoli, S., Silva, V., Sheidaei, S., &Alimardani, R. (2023). CFD and response surface methodology coupling for optimization of a duct used in ducted wind turbines. *Heliyon, 9*(6), e17057. https://doi.org/10.1016/j.heliyon.2023.e17057
14. Vaz, J. R. P., & Wood, D. H. (2018). Effect of the diffuser efficiency on wind turbine performance. *Renewable Energy, 126*, 969–977. https://doi.org/10.1016/j.renene.2018.04.013
15. Wood, D. (2011). *Small wind turbines: Analysis, design, and application*. Springer. https://doi.org/10.1007/978-1-84996-175-2

Conflict of Interest Statement: *The authors declare that there is no conflict of interest regarding the publication of this paper.*

Generative AI Statement: *The author(s) confirm that no Generative AI tools were used in the preparation or writing of this article.*

Publishers Note: *All statements made in this article are the sole responsibility of the authors and do not necessarily reflect the views of their affiliated institutions, the publisher, editors, or reviewers. Any products mentioned or claims made by manufacturers are not guaranteed or endorsed by the publisher.*

Cite this Article

Tarun Kumar Ahirwar, Paulami Sahu, Prashant V. Baredar. Preliminary CFD Evaluation of Selected Hypotheses for a Wind Energy Concentrator. International Research Journal of Engineering & Applied Sciences (IRJEAS). 12(4), pp. 01-11, 2025. https://doi.org/10.55083/irjeas.2025.v13i04001